

## Diode laser spectrometer at 493 nm for single trapped Ba<sup>+</sup> ions

C. Raab, J. Bolle, H. Oberst, J. Eschner, F. Schmidt-Kaler, R. Blatt

Institut für Experimentalphysik, Universität Innsbruck, Technikerstraße 25, A-6020 Innsbruck, Austria

Received: 12 June 1998

**Abstract.** A diode laser spectrometer at 493 nm is described, which is especially suited for spectroscopy of single trapped Ba<sup>+</sup> ions. Frequency doubling of a 100 mW diode laser at 986 nm results in up to 60 mW output power at 493 nm in a bandwidth of less than 60 kHz with respect to the cavity used for locking. Reference frequencies of 18 spectral lines of Te<sub>2</sub> near the 493 nm resonance of Ba<sup>+</sup> have been measured using modulation transfer spectroscopy. The fluorescence excitation spectrum of a single Ba<sup>+</sup> ion, measured with this laser, exhibits well-resolved dark resonances, which confirms the versatility of the system for quantum optical experiments.

**PACS:** 39.30.+w; 42.60.By; 42.80.Pj; 33.20.Kf

Single trapped ions have played a major role in the development of quantum optics since their first demonstration in 1980 [1]. In particular, they have been applied to fundamental investigations of the interaction between light and matter [2, 3], to ultrahigh precision spectroscopy, and to the development of frequency standards [4]. Present and future applications involve the generation and measurement of quantum states, in particular in the framework of quantum information and quantum computing [5], with our short-term application being the study of the ion's state by spectral analysis of its resonance fluorescence. In such experiments lasers are used to optically cool the ion and to control and measure its quantum state, i.e., the internal electronic state and the motional state of the trapped ion are manipulated with near-resonant laser light. A generic level scheme that applies to several elements typically used in single ion traps (such as Ca<sup>+</sup>, Ba<sup>+</sup>, and Sr<sup>+</sup>), consists of an S<sub>1/2</sub>, P<sub>1/2</sub> and a metastable D<sub>3/2</sub> state in lambda configuration. In this case, two lasers are necessary to continuously cool the ion and generate resonance fluorescence, one for the S–P transition and one for the D–P transition. Since reliable cooling and state preparation is a prerequisite for all the above-mentioned applications, these lasers have to be stabilized against long-term drift and their linewidths have to be reduced to a level below the typical frequencies involved, such as the Zeeman splitting (≈ 5 MHz), the vibrational frequency in the trap (≈ 1 MHz), and the width of

Raman resonances which appear in the lambda level scheme (≈ 0.1 MHz) [6]. Spectral analysis of the single ion's fluorescence is also facilitated if the laser, which determines the width of the elastic component, is spectrally narrow.

The very first single-ion experiments were carried out with barium [1] because dye lasers at 493 nm (S–P) and 650 nm (P–D) were available at that time; Fig. 1 shows the relevant levels of the barium ion. Dye lasers have a large tuning range and can be stabilized well. Their disadvantages are their difficult handling and, due to the need for an ion pump laser, their high acquisition and running costs. Today, with the availability of diode lasers in many spectral regimes, more and more experiments utilize these low-cost and robust lasers. Although the first diode lasers were delicate to handle and their spectral qualities were poor, progress in the production process has made them much more reliable and has led to a vast improvement of their optical characteristics. The average lifetime of diode lasers now ranges from 10 000 h, up to several 100 000 h, which exceeds the lifetime of ion lasers by far. Their spectral purity can be improved using various optical feedback schemes as well as electronic stabilization.

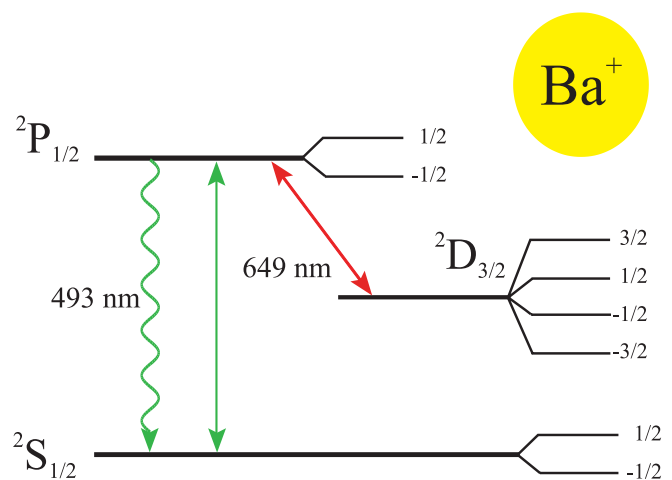


**Fig. 1.** Level scheme of <sup>138</sup>Ba<sup>+</sup> with Zeeman level splitting schematically indicated

Currently, there are still no laser diodes commercially available with wavelengths below 600 nm. Therefore, in order to reach the spectral range down to 400 nm, one can use frequency doubling in external cavities [7–10]. In this paper we describe a diode laser system that provides powerful, tunable, and frequency-stable light at 493 nm, which is used for quantum optics and precision spectroscopy with single  $\text{Ba}^+$  ions. Light of a 986 nm laser diode ( $P_{\text{max}} = 150 \text{ mW}$ ), which is stabilized by optical feedback from a grating, is frequency-doubled with a  $\text{KNbO}_3$  crystal in an external cavity where a maximum conversion efficiency of 63% is achieved.

For a first demonstration of the spectroscopic qualities of the 493 nm laser system and in order to find stable frequency markers independent of  $\text{Ba}^+$ , we carried out Doppler-free spectroscopy on molecular tellurium at wavelengths near the S–P transition of  $\text{Ba}^+$  (493.54 nm). To obtain a clean Doppler-free signal, we used modulation transfer spectroscopy (MTS) [11–13]. 18  $\text{Te}_2$  lines were found near the barium resonance in the range from  $20261.46 \text{ cm}^{-1}$  to  $20261.87 \text{ cm}^{-1}$ . The closest line is approximately 330 MHz above the  $\text{Ba}^+$  transition, a frequency difference that can be easily bridged with an acousto-optical modulator (AOM).

As a first application to a single  $\text{Ba}^+$  ion, we recorded the fluorescence excitation spectrum obtained by scanning the 493 nm laser over the S–P resonance, with another diode laser exciting the P–D transition (650 nm) at a fixed frequency. Well-resolved dark resonances are observed in the fluorescence in agreement with theoretical predictions and with earlier observations. The paper is organized as follows: In Sect. 1 the experimental setup is presented: generation of well-stabilized laser light at 986 nm and frequency doubling in an external enhancement cavity with high efficiency. In Sect. 2 modulation transfer spectroscopy of  $\text{Te}_2$  is described and in Sect. 3 the application of this light source for quantum optical measurements on a single  $\text{Ba}^+$  ion is demonstrated.

## 1 Laser system

The laser system consists of three main parts, the diode laser at 986 nm, the stabilization to a reference cavity, and the frequency doubler. The experimental setup is shown in Fig. 2. An SDL 6500 laser diode (150 mW) is temperature stabilized and driven with a commercial current source (ILX LDX-3620). The emitted light is vertically polarized and collimated into a parallel beam with an  $f = 5 \text{ mm}$  triplet lens. To reduce the large inherent emission bandwidth and to select the lasing wavelength, we use optical feedback from a grating. We have chosen a setup in the Littman–Metcalf configuration [14], which has several advantages compared with the more commonly used Littrow scheme. These are, for example, the fixed output beam position and the adjustable feedback level. The laser beam illuminates the grating (1800 lines/mm, 30 mm long) at an angle of about  $75^\circ$  to obtain high wavelength selectivity and a high output coupling rate, emitting 89% into the 0th order. About 4% of the power is diffracted into the 1st order which is back reflected from a mirror into the laser diode. The laser operates in a single mode at an output power of up to 130 mW with 200 mA injection current. The emission wavelength of the laser can be adjusted between 976 nm and 990 nm by tilting the mirror. The laser frequency is fine

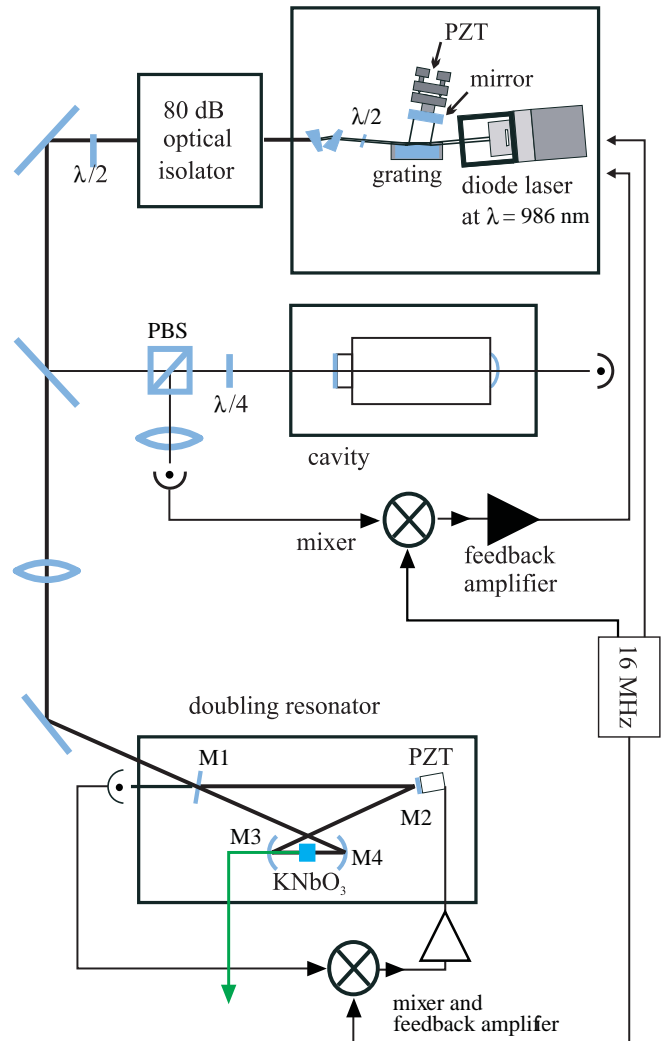


Fig. 2. Laser setup showing the IR laser, the stabilization circuit, and the frequency doubler

tuned by shifting the mirror along the  $z$  axis with a high voltage applied to the piezo ceramic (PZT, see Fig. 2). Thus we obtain a continuous tuning range of 1.5 GHz. Using additional feed-forward adjustment of the injection current, the continuous tuning range increases to 3 GHz. The polarization of the output light is rotated  $90^\circ$  with a half-wave plate to avoid losses at the anamorphic prism pair, which is used to circularize the beam. Unwanted feedback into the diode laser from the rest of the experimental setup is prevented with two Faraday isolators of 40 dB isolation each.

The laser is actively locked to a reference cavity using a Pound–Drever–Hall stabilization scheme [15]. The cavity has a finesse of 1200 and a free spectral range of 1.2 GHz, its drift rate is about 0.5 MHz/min. FM sidebands of about  $10^{-4}$  of the laser power are generated by modulating the laser diode injection current at 16 MHz. A small part ( $\approx 2\%$ ) of the laser light is coupled into the reference cavity, and the reflected light is separated, using a quarter-wave plate and a polarizing beam splitter, and detected with a fast photodiode. The photo current is mixed with the 16-MHz reference to produce an error signal, which is amplified with a PID amplifier and fed back to the diode current and the piezo-mounted Littman mir-

ror. We achieve a short-term ( $\tau < 1$  s) laser linewidth below 30 kHz rms with respect to the reference cavity. For scanning, the frequency of the locked laser is varied by tuning the reference cavity with a piezo.

Frequency doubling of the diode laser light is achieved with a  $\text{KNbO}_3$  crystal, which is placed inside an enhancement cavity for the 986 nm light. This ring cavity consists of two plane mirrors and two curved mirrors of 38 mm radius. Three mirrors (M2, M3, M4) have high reflectivity at 986 nm,  $R > 99.9\%$ , and they transmit about 95% at 493 nm. The input coupler (M1) is chosen to have a reflectivity of  $R = 97\%$ , which leads to an impedance matching of better than 80% at optimum doubling efficiency. The resonator length is 395 mm and the distance between the curved mirrors is 82 mm. Mirror M2 is mounted on a PZT to tune the resonator length. The 5 mm B-cut  $\text{KNbO}_3$  crystal is placed between the curved mirrors and the cavity is designed for an optimum focus inside the crystal [16]. The 986 nm laser light is mode matched, with a single lens, into the doubling cavity. We achieve 90% mode matching efficiency into  $\text{TEM}_{00}$ . The doubling cavity is locked, also with a Pound–Drever–Hall feedback circuit, to the frequency of the IR laser using the 16-MHz sidebands on the 986 nm light. The error signal is fed back to the piezo-mounted mirror M2. This mirror has a diameter 6.75 mm and 3 mm thickness. In combination with a fast piezo we obtain a servo-loop bandwidth of about 40 kHz. Together with a 12 dB/octave integrator this leads to an intensity stability of the frequency-doubled light of better than  $2 \times 10^{-3}$  under normal laboratory background noise conditions.

At a diode current of 200 mA we obtain 94 mW light at 986 nm in front of the doubler and up to 60 mW of green light out of the doubling cavity. This corresponds to 63% conversion efficiency of the frequency doubler. The overall efficiency, i.e. the ratio of the electrical power injected into the diode to the output power of the green light amounts to 16%.

## 2 Spectroscopy on $\text{Te}_2$

The experimental setup for spectroscopy of  $\text{Te}_2$  is shown in Fig. 3. We use modulation transfer spectroscopy (MTS), a Doppler-free method that detects a rf modulation of a probe beam which is generated in the  $\text{Te}_2$  vapor via four-wave-mixing with a counter-propagating, rf-modulated pump beam [11, 13, 17–19]. The advantage of this technique in comparison to frequency modulation spectroscopy (FMS) [20–22] is that the Doppler-free spectra appear without a background slope and therefore, the resulting signals can be used for locking a diode laser directly to the molecular resonance without the need for offset compensation. The laser light is divided into the pump and the probe beam with a polarizing beam splitter. The splitting ratio is adjusted with a half-wave plate to optimize the signal-to-noise ratio. The pump beam is frequency-modulated with a  $\text{LiTaO}_3$  electro-optical modulator (EOM) driven at 6 MHz frequency. The EOM is heated to about 100 °C to avoid optical damage of the crystal. As shown in Fig. 3, the pump and the probe beam counter-propagate with orthogonal polarizations through the  $\text{Te}_2$  cell, which is heated to about 420 °C. The beams are focused with  $f = 200$  mm lenses to increase the intensity inside the cell and the probe beam is detected with a fast photodiode whose output is amplified and mixed with the 6 MHz reference using a double-balanced mixer. The phase of the local oscillator can be shifted over a range of 360°, and the MTS signal is recorded with a Tektronix TDS784 oscilloscope.

We have scanned the spectral range from  $20\,261.46\text{ cm}^{-1}$  to  $20\,261.87\text{ cm}^{-1}$  in several intervals of  $\approx 2.5$  GHz with the laser locked to the reference cavity. Neighboring scans overlap and were taken with at least one common  $\text{Te}_2$  resonance. In order to obtain a frequency scale, a small part of the green light was coupled into a Fabry–Pérot resonator (FP2) with a free spectral range of 725.6(1) MHz.

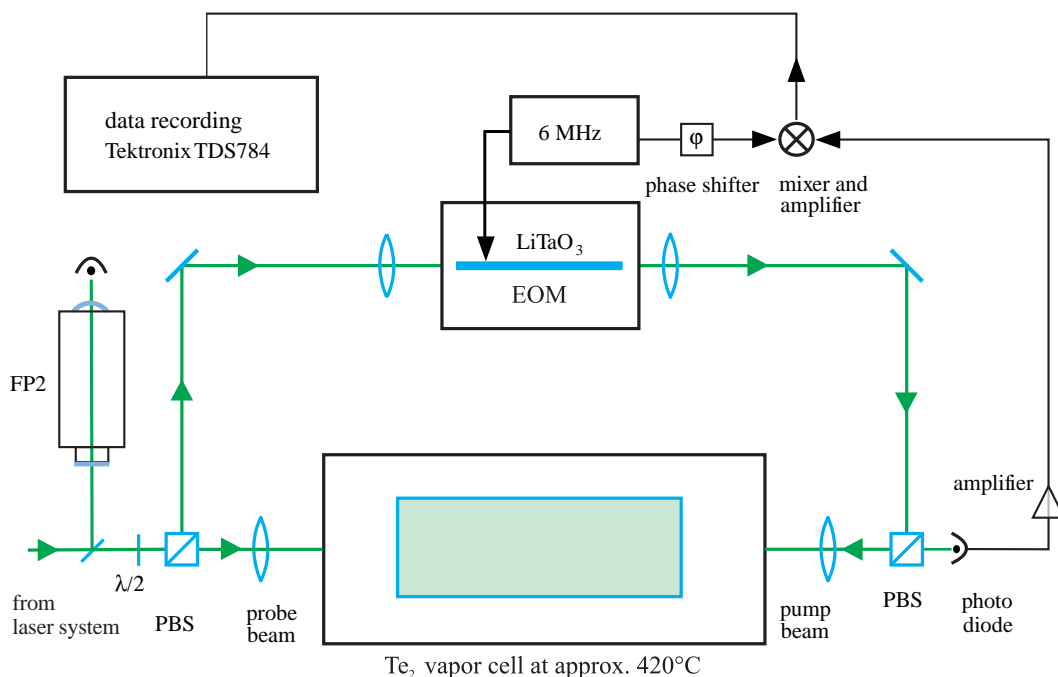


**Fig. 3.** Schematic setup for modulation transfer spectroscopy of  $\text{Te}_2$

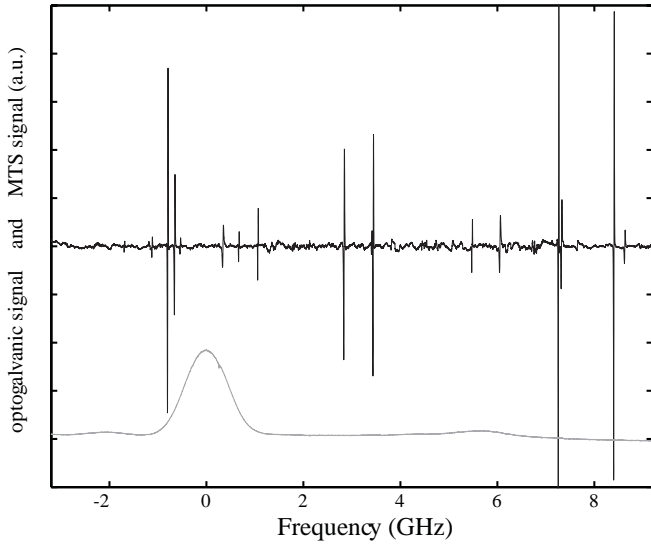


**Fig. 4.** Upper curve: Te<sub>2</sub> spectrum from 20261.46 cm<sup>-1</sup> to 20261.87 cm<sup>-1</sup>. Lower curve: Ba<sup>+</sup> optogalvanic spectrum

The frequency axis has been calibrated from the measured cavity resonances with 1% relative accuracy, limited by the nonlinearity of the scanning piezo and the drift of the cavity. The absolute wavelengths were determined with a wavemeter and by means of optogalvanic spectroscopy of Ba<sup>+</sup> which has been carried out simultaneously. The measured spectra are shown in Fig. 4. From a Gaussian fit to the measured Ba<sup>+</sup> spectrum the center of the S–P resonance at 493 nm was determined with an accuracy of 26 MHz. The literature value of this resonance frequency, 20261.562 cm<sup>-1</sup> [23], was taken as the absolute frequency reference. In the covered frequency range of 12.7 GHz, 18 tellurium resonances were resolved. Their positions and relative amplitudes are listed in Table 1. By comparison with the Tellurium Atlas of Cariou and Luc [24], two of their lines, No. 3435 (20261.5342 cm<sup>-1</sup>) and No. 3436 (20261.8012 cm<sup>-1</sup>), were identified as our No. 3 and 14. The measured distance of 8.06(8) GHz between these two lines is in good agreement with the listed separation of 0.2670 cm<sup>-1</sup>. The smallest fre-

quency distance between one of the Te<sub>2</sub> lines (line No. 6 in Table 1) and the Ba<sup>+</sup> resonance is 330 MHz. For further investigation we concentrated on the strong line No. 3435 (No. 14 in Table 1). Scanning 100 MHz about this line was used to resolve the MTS line shape and compare it to the theoretically expected shapes [18, 25]. For a calculation of the latter, and for low modulation index as in our experiment, only the first sideband has to be taken into account and the line shape of the demodulated signal is given by:

$$S(\Delta) = \text{Re} \left[ \sum_{j=a,b} \frac{\mu_{ab}^2}{\gamma_j + i\delta} \left( \frac{1}{\gamma_{ab} + i(\Delta + \delta/2)} - \frac{1}{\gamma_{ab} + i(\Delta + \delta)} + \frac{1}{\gamma_{ab} - i(\Delta - \delta)} - \frac{1}{\gamma_{ab} - i(\Delta - \delta/2)} \right) e^{-i\vartheta} \right]. \quad (1)$$

Here,  $a$  and  $b$  denote the lower and the upper level of the Te<sub>2</sub> transition, respectively,  $\mu_{ab}$  is the electric dipole moment,  $\Delta = \omega_{\text{laser}} - \omega_{ab}$  is the detuning of the laser,  $\gamma_{a,b}$  are the decay rates of the two levels,  $\gamma_{ab}$  is the optical relaxation rate from  $a$  to  $b$ ,  $\delta$  is the modulation frequency, and  $\vartheta$  is the demodulation phase. The measured data have been fitted with this line shape. Figure 5 shows the data and the fit for phases 95° and 180°. The fitting parameters are  $\gamma_{ab}$ ,  $\vartheta$ , a scaling factor proportional to  $\sum_{j=a,b} \mu_{ab}^2 / (\gamma_j + i\delta)$  and the frequency offset. The fitting procedure yields a linewidth of the measured line of  $\gamma_{ab} = 3.9(2)$  MHz. The asymmetry in the experimental data is attributed to a residual amplitude modulation in the EOM.

### 3 Spectroscopy of a single Ba<sup>+</sup> ion

For spectroscopy of single trapped Ba<sup>+</sup> ions, an additional laser at 650 nm is required to excite the D–P transition. The setup of this laser uses a SDL 7511 laser diode and is otherwise very similar to the setup of the infrared diode laser. The ion is stored in a miniature Paul trap and localized to

**Table 1.** Positions and relative amplitudes of lines in the Te<sub>2</sub> spectrum. The amplitude has been defined by the difference between the maximum and the minimum signal at 90° demodulation phase. Lines No. 3 and 14 have been previously published in [24]. The errors in frequency are the relative errors of the scaling, the errors in wave number are absolute errors

Line number	Relative frequency /GHz	Wave number /cm <sup>-1</sup>	Relative amplitude
1	-1.70(1)	20261.505(1)	0.8
2	-1.13(1)	20261.524(1)	1.4
3	-0.808(8)	20261.535(1)	23.9
4	-0.666(6)	20261.540(1)	9.7
5	-0.549(5)	20261.544(1)	1.1
6	0.330(3)	20261.573(1)	2.9
7	0.658(6)	20261.584(1)	2.1
8	1.05(1)	20261.597(1)	5.0
9	2.83(2)	20261.656(2)	14.6
10	3.40(3)	20261.675(2)	1.6
11	4.01(4)	20261.696(2)	16.7
12	5.47(4)	20261.744(3)	3.7
13	6.05(6)	20261.764(3)	3.9
14	7.25(7)	20261.804(3)	78.0
15	7.31(7)	20261.806(3)	5.5
16	7.64(7)	20261.817(3)	0.7
17	8.39(8)	20261.842(4)	32.4
18	8.61(8)	20261.850(4)	2.3

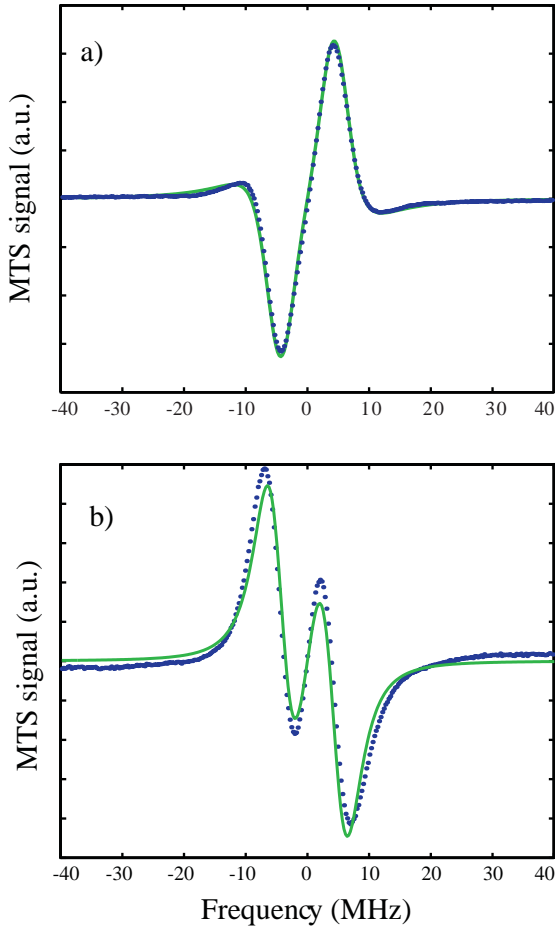


Fig. 5. Line No. 3435 with high resolution (*points*) and calculated MTS line shape (*solid line*)

better than a few  $\mu\text{m}$ . The light from the two lasers is combined using a dichroic mirror and focused into the trap with an  $f=250$  mm lens resulting in a diameter of the focus in the trap center of  $\approx 80$   $\mu\text{m}$ . The light level is adjusted using a half-wave plate and a polarizer. Three orthogonal pairs of Helmholtz coils are employed to produce a well-defined magnetic field that is oriented perpendicular to the direction of light polarization. Fluorescence from the ion is collected with an  $f/0.7$  quartz collimator, imaged onto a cooled photomultiplier, and recorded in photon-counting mode for 0.1 s per data point. For continuous excitation of fluorescence, the laser at 493 nm has to be tuned below the S–P resonance to maintain optical cooling of the ion [26–28]. Figure 6 shows a scan of the laser at 493 nm across the  $\text{Ba}^+$  resonance in steps of  $\approx 100$  kHz while the laser at 650 nm is kept at a fixed frequency below the D–P resonance. The power of the green light was set to 25  $\mu\text{W}$ , the red power is 9  $\mu\text{W}$ . The frequency axis is calibrated with the help of an optogalvanic signal from a barium hollow cathode lamp, which is recorded simultaneously with the  $\text{Ba}^+$  fluorescence. Four dark resonances are resolved in the fluorescence signal. These occur when the detuning for an S–D Raman transition between one of the Zeeman sublevels becomes zero [6]. The solid line in Fig. 6 indicates a fitted curve to the measured data calculated from 8-level Bloch equations taking into account the Zeeman substructure of the S, P, and D levels, the light polarization, and

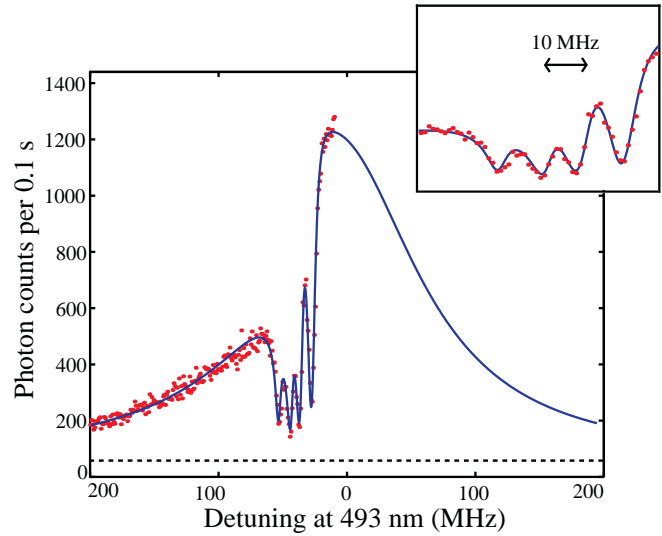


Fig. 6. Fluorescence excitation spectrum of a single trapped  $\text{Ba}^+$  ion, experimental data (*points*) and calculated fit (*line*). The *dashed line* indicates the constant background count rate. The *insert* shows the four dark resonances magnified, with background subtracted

magnetic field [29]. The complex spectral shape is well reproduced in the calculation. In particular, the measured and calculated widths and depths of the dark resonances, which are determined by the laser intensities and linewidths, respectively, agree well. Experimental parameters determined from the fit are the green and red light intensity, the exact detuning of the red laser, the magnetic field, the angle between magnetic field and light polarization, and the common linewidth of both lasers. The intensities are 380(50)  $\text{mW}/\text{cm}^2$  at 493 nm and 140(20)  $\text{mW}/\text{cm}^2$  at 650 nm. The magnetic field is  $5.8(3) \times 10^{-4}$  Tesla, the angle is  $88(7)^\circ$ , the detuning of the red laser is  $-40.6(7)$  MHz, and the common linewidth of both lasers is 89(35) kHz. If we assume that both lasers have the same width, the linewidth of the laser at 493 nm is 63 kHz, which agrees well with the value measured from the error signal.

#### 4 Conclusion

We have set up a powerful, frequency-stable and reliable laser system for spectroscopy of single  $\text{Ba}^+$  ions. We obtain a maximum output power of 60 mW of light at 493 nm in a bandwidth of 60 kHz rms. Doppler-free modulation transfer spectroscopy was carried out on molecular tellurium and 18 lines were found in a spectral region of 8 GHz around the  $\text{Ba}^+$   $S_{1/2} - P_{1/2}$  transition. The MTS signal agrees well with theory. In order to eliminate the cavity drift in the laser stabilization circuit, the laser will be actively locked to the  $\text{Te}_2$  line, which is 330 MHz above the  $\text{Ba}^+$  S–P transition, and the laser frequency will be scanned with an acousto-optical modulator. We have applied the laser to excite resonance fluorescence from a single  $\text{Ba}^+$  ion in a Paul trap. Well-resolved dark resonances and a spectral line shape that agrees well with the theory confirm the versatility of the laser system for quantum optical measurements.

*Acknowledgements.* This work is supported by the Fonds zur Förderung der wissenschaftlichen Forschung (FWF) under contract number P11467-PHY and in parts by the TMR network “Quantum Structures” (ERB-FMRX-CT96-0077).

## References

1. W. Neuhauser, M. Hohenstatt, P.E. Toschek, H.G. Dehmelt: *Phys. Rev. A* **22**, 1137 (1980)
2. D.M. Meekhof, C. Monroe, B.E. King, W.M. Itano, D.J. Wineland: *Phys. Rev. Lett.* **76**, 1796 (1996)
3. C. Monroe, D.M. Meekhof, B.E. King, D.J. Wineland: *Science* **272**, 1131 (1996)
4. R. Blatt: In *Atomic Physics* **14**, p. 219, ed. by D.J. Wineland, C.E. Wieman, S.J. Smith (AIP, New York 1995)
5. J.I. Cirac, P. Zoller: *Phys. Rev. Lett.* **74**, 4091 (1995)
6. I. Siemers, M. Schubert, R. Blatt, W. Neuhauser, P.E. Toschek: *Europhys. Lett.* **18**, 139 (1992)
7. P. Lodahl, J.L. Sørensen, E.S. Polzik: *Appl. Phys. B* **64**, 383 (1997)
8. W.J. Kozlovsky, W. Lentz, E.E. Latta, A. Moser, G.L. Bona: *Appl. Phys. Lett.* **56**, 2291 (1990)
9. A.S. Zibrov, R.W. Fox, R. Ellingsen, C.S. Weimer, V.L. Velichansky, G.M. Tino, L. Hollberg: *Appl. Phys. B* **59**, 327 (1994)
10. C. Zimmermann, V. Vuletic, A. Hemmerich, T.W. Hänsch: *Appl. Phys. Lett.* **66**, 2318 (1995)
11. L.S. Ma, Ph. Courteille, G. Ritter, W. Neuhauser, R. Blatt: *Appl. Phys. B* **57**, 159 (1993)
12. J.L. Hall, R. Felder, L.S. Ma: Conference on Precision Electromagnetic Measurements, Paris (1992) p. 160
13. J.J. Snyder, R.K. Kaj, D. Bloch, M. Ducloy: *Opt. Lett.* **5**, 163 (1980)
14. K.C. Harvey, C.J. Myatt: *Opt. Lett.* **16**, 910 (1991)
15. R.W.P. Drever, J.L. Hall, F.V. Kowalski, J. Hough, G.M. Ford, A.J. Munley, H. Ward: *Appl. Phys. B* **31**, 97 (1983)
16. G.D. Boyd, D.A. Kleinman: *J. Appl. Phys.* **39**, 3597 (1968)
17. R.K. Kaj, D. Bloch, J.J. Snyder, G. Camy, M. Ducloy: *Phys. Rev. Lett.* **44**, 1251 (1980)
18. G. Camy, D. Bloch: *J. Phys.* **43**, 57 (1982)
19. A. Schenzle, R.G. DeVoe, R.G. Brewer: *Phys. Rev. A* **25**, 2606 (1982)
20. M.D. Levenson, G.L. Eesley: *Appl. Phys.* **19**, 1 (1979)
21. G.C. Bjorklund: *Opt. Lett.* **5**, 15 (1980)
22. J.L. Hall, L. Hollberg, T. Baer, H.G. Robinson: *Appl. Phys. Lett.* **39**, 680 (1981)
23. Ch. Moore: *Atomic Energy Levels, Volume III*, NIST (1971)
24. J. Cariou, P. Luc: *Atlas du Spectre d'Absorption de la molécule de Tellure*, Laboratoire Aimé-Cotton, CNRS II, Orsay, France (1980)
25. L.S. Ma, L.E. Ding, Z.Y. Bi: *Appl. Phys. B* **51**, 233 (1990)
26. W. Neuhauser, M. Hohenstatt, P.E. Toschek, H.G. Dehmelt: *Phys. Rev. Lett.* **41**, 233 (1978)
27. D.J. Wineland, R.E. Drullinger, F.L. Walls: *Phys. Rev. Lett.* **40**, 1639 (1978)
28. D. Reiß, A. Lindner, R. Blatt: *Phys. Rev. A* **54**, 5133 (1996)
29. M. Schubert, I. Siemers, R. Blatt, W. Neuhauser, P.E. Toschek: *Phys. Rev. A* **52**, 2994 (1995)